

Dynamical control and novel quantum phases in impurity doped linear ion crystals

Peter A. Ivanov,^{1,2} Nikolay V. Vitanov,² Kilian Singer,¹ and Ferdinand Schmidt-Kaler¹

¹*Institut für Quanteninformationsverarbeitung, Universität Ulm, Albert-Einstein-Allee 11, 89081 Ulm, Germany*

²*Department of Physics, Sofia University, James Bourchier 5 blvd, 1164 Sofia, Bulgaria*

(Dated: November 2, 2018)

We explore the behavior of the phonon number distribution in an heterogeneous linear ion crystal. The presence of ion species with different masses changes dramatically the transverse energy spectrum, in such a way that two eigenfrequencies become non-analytic functions of the mass ratio in the form of a sharp cusp. This non-analyticity induces a quantum phase transition between condensed and conducting phase of the transverse local phonons. In order to continuously vary the mass ratio we adiabatically modify a locally applied laser field, exerting optical dipole forces which reduces the effective mass.

PACS numbers: 03.67.Ac, 37.10.Ty, 64.70.Tg, 73.43.Nq

I. INTRODUCTION

Trapped ions are one of the most attractive physical systems for implementing quantum computation [1] and quantum simulation [2]. The ability to control and measure the internal and external degrees of freedom with high accuracy allows for experimental implementations of various quantum gates [3–6] and quantum computing protocols [7–9]. Trapped ions represent a convenient system for the simulation of many-body effects, such as quantum phase transitions in spin systems [10, 11], atoms in optical lattices [12] and coupled cavity arrays [13]. Recently, a simulation of the Dirac equation for a free spin-1/2 particle [14] has been successfully performed with a single trapped ion [15].

While small, homogeneous ion crystals have been extensively studied, the novelty of this paper is elucidating the richness of quantum phases in ion crystals doped with a second ion species. Depending on the mass ratio, the crystal allows for the observation of two quantum phases of the transverse *local* phonon number distribution. For a heavy impurity ion all phonons are condensed by the latter and the variance of the transverse local phonon distribution is zero. At the same time zero average phonons with vanishing variance and correlation are observed at all other sites. In the following this state is referred to as the quantum *condensed* phase. In the opposite case, if a lighter impurity ion is added, the system is in a quantum *conducting* phase [12] where the phonons are redistributed among all ions showing non-zero variance and correlation, while the average phonons of the impurity ion is significantly reduced. There are two ways to vary the mass ratio in heterogeneous ion crystal. The first one is by doping a mono-species ion crystal with one impurity ion, a technique which has been applied for ion frequency standards [16], sympathetic cooling of molecular ions [17], and for deterministic ion implantation [18]. The second scheme overcomes this discrete, stepwise variation and uses optical dipole forces by non-resonant tightly focused laser beams [19] (Fig. 1). It is still advantageous to use heavier doping ions because the dipole force can only reduce the effective mass but to observe the phase

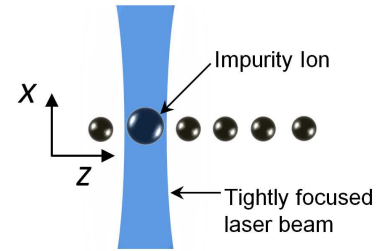


FIG. 1: (color online). Impurity-doped linear ion crystal consisting of ions with mass m and an impurity ion with mass M . The mass ratio $\mu = M/m$ determines the two quantum phases. Applying a tightly focused laser field to the impurity ion in the transverse x direction makes it possible to continuously vary the effective mass ratio. Increasing the magnitude of the light field leads to a decrease of the effective mass.

transition the critical point of unity mass ratio has to be crossed. Current ion trap technology allows to implement all crucial elements of the proposal: preparation of the initial state, laser-ion interaction driving the dynamics required for the quantum phase transition, and readout of the phonon distribution.

II. TRANSVERSE ENERGY SPECTRUM

In the following we first consider a harmonically confined ion crystal with $N - 1$ ions of mass m and one impurity ion of mass M at position j_M without any focused laser field. If the radial confinement is stronger than the axial one then ions are arranged in a linear ion crystal along the axial z axis and occupy equilibrium positions z_i^0 . Since the axial trap potential is independent of the mass, the equilibrium positions $z_i^0 = lu_i$ of the ions are independent of the composition of the ion crystal. Here l is the natural length scale and u_i are dimensionless equilibrium positions [20]. The transverse, dynamic Paul confinement along x and y directions is generated by an applied radio frequency (RF) quadrupole field. In the following we only consider one transverse

direction x . The oscillation frequency in x direction is $\omega_x^0 = |e|U_{\text{RF}}c_x/(\sqrt{2}m\Omega_{\text{RF}})$, where U_{RF} is the amplitude of the RF voltage with frequency Ω_{RF} , e is the electron charge and c_x is a geometry factor. The transverse oscillation frequency is additionally reduced by the axial trap frequency ω_z according to $\omega_x = \omega_x^0(1 - \alpha^2/2)^{1/2}$, in lowest-order approximation, where $\alpha = \omega_z/\omega_x^0$ [21]. For a small displacement the motional degrees of freedom in x , y and z direction are decoupled. The normal mode eigenfrequencies $\omega_k = \omega_x^0\sqrt{\lambda_k}$ and eigenvectors b_j^k are obtained from the diagonalization of a matrix B_{ij} with $\sum_i B_{ij}b_i^k = \lambda_k b_j^k$, where ω_x^0 is the transverse frequency of a single ion with mass m . The real and symmetric N -dimensional matrix B_{ij} is determined by the harmonic expansion of the external trapping potential and the Coulomb interaction between the ions; it reads [22]

$$B_{ij} = \begin{cases} 1 - \frac{\alpha^2}{2} - \alpha^2 \sum_{p \neq j}^N \frac{1}{|u_j - u_p|^3}, & (i = j, j \neq j_M), \\ \frac{1}{\mu^2} - \frac{\alpha^2}{2\mu} - \frac{\alpha^2}{\mu} \sum_{p \neq j}^N \frac{1}{|u_j - u_p|^3}, & (i = j = j_M), \\ \frac{\alpha^2}{|u_i - u_j|^3}, & (i \neq j \neq j_M), \\ \frac{\alpha^2}{\sqrt{\mu}|u_i - u_j|^3}, & (i \neq j = j_M), \end{cases} \quad (1)$$

where $\mu = M/m$ denotes the mass ratio of both ion species. By expressing the position and momentum operators in terms of normal phonon modes

$$\hat{x}_j = \sum_k b_j^k \hat{X}_k, \quad \hat{p}_j = \sum_k b_j^k \hat{P}_k, \\ \hat{x}_{j_M} = \frac{1}{\sqrt{\mu}} \sum_k b_{j_M}^k \hat{X}_k, \quad \hat{p}_{j_M} = \sqrt{\mu} \sum_k b_{j_M}^k \hat{P}_k, \quad (2)$$

the Hamiltonian takes the form $\hat{H}_0 = \sum_k \hbar\omega_k(\hat{N}_k + 1/2)$. Here $\hat{X}_k = \sqrt{\hbar/2m\omega_k}(\hat{a}_k^\dagger + \hat{a}_k)$ is the normal mode position operator and $\hat{P}_k = i\sqrt{\hbar m\omega_k/2}(\hat{a}_k^\dagger - \hat{a}_k)$ is the normal mode momentum operator, while \hat{a}_k^\dagger and \hat{a}_k are the phonon creation and annihilation operators of the k th collective phonon mode and $\hat{N}_k = \hat{a}_k^\dagger \hat{a}_k$ is the respective *collective* phonon number operator.

In order to visualize the transverse mode we plot in Fig. 2 the eigenfrequencies ω_k for a string of six ions, with an impurity ion at position $j_M = 2$ when the mass ratio is varied. As μ increases beyond unity, the frequency spacing between the lowest-lying energy mode (LL) with frequency ω_N and all other modes increases, while for $\mu < 1$ it tends towards degeneracy. In the transverse direction the highest energy mode, the center-of-mass mode (COM) with frequency ω_1 , is nearly degenerate for $\mu > 1$. When μ decreases below the value $\mu = 1$ the frequency spacing between COM mode and all other modes increases. In real experiments the mass ratio can only be changed to discrete values as shown in Fig. 2.

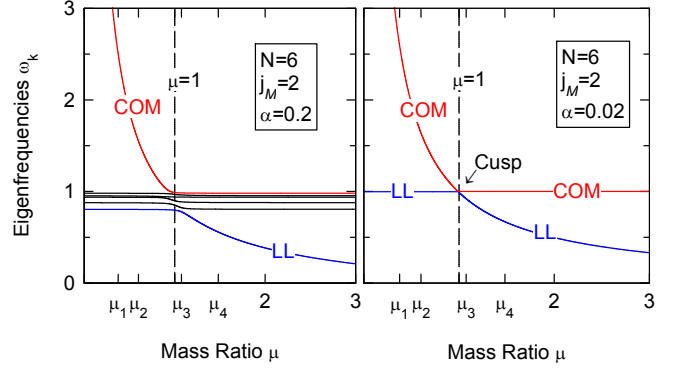


FIG. 2: (color online). Normalized transverse eigenfrequencies $\omega_k/\omega_x^0 = \sqrt{\lambda_k}$ when μ is varied. The highest energy center-of-mass (COM) and the lowest-lying (LL) modes are shown. Different ion species are depicted as follows: $\mu_1 = {}^9\text{Be}^+ / {}^{24}\text{Mg}^+$, $\mu_2 = {}^{24}\text{Mg}^+ / {}^{40}\text{Ca}^+$, $\mu_3 = {}^{40}\text{Ca}^+ / {}^{43}\text{Ca}^+$ and $\mu_4 = {}^{40}\text{Ca}^+ / {}^{27}\text{Al}^+$. b) Decreasing α the LL and COM modes develop a cusp at $\mu = 1$.

However, later in the paper we show how to overcome this limitation by optical forces.

As α is decreased the gap at the avoided level-crossing ($\mu = 1$) between the modes vanishes. Moreover, LL and COM modes develop a cusp at $\mu = 1$. For sufficiently small $\alpha \ll 1$ the off-diagonal elements of B_{ij} (1) can be neglected and the eigenfrequencies ω_k behave as follows

$$\left. \begin{array}{l} \omega_1 \rightarrow \frac{\omega_x}{\mu} \\ \omega_{n \neq 1} \rightarrow \omega_x \end{array} \right\} \text{ for } \mu < 1, \quad \left. \begin{array}{l} \omega_{n \neq N} \rightarrow \omega_x \\ \omega_N \rightarrow \frac{\omega_x}{\mu} \end{array} \right\} \text{ for } \mu > 1.$$

This implies that the COM frequency ω_1 and the LL frequency ω_N , respectively, have discontinuous derivatives at $\mu = 1$. Therefore, the non-analyticity of the ground state energy indicates a quantum phase transition [23]. We will exemplify the properties of the two quantum phases by calculating the phonon number distribution, its variance and correlation. These quantities are all experimentally accessible by laser-spectroscopy measurements.

III. QUANTUM PHASES

The characteristic feature of the quantum phase transition is expressed clearly by the behavior of the *local* phonon number operator

$$\hat{n}_j = \frac{m\omega_x^0(m)}{2\hbar} \hat{x}_j^2 + \frac{\hat{p}_j^2}{2\hbar m\omega_x^0(m)} - \frac{1}{2}, \\ \hat{n}_{j_M} = \frac{M\omega_x^0(M)}{2\hbar} \hat{x}_{j_M}^2 + \frac{\hat{p}_{j_M}^2}{2\hbar M\omega_x^0(M)} - \frac{1}{2}. \quad (3)$$

Initially the mixed ion crystal is prepared by laser-ion interactions in the state with n phonons in the LL collective mode and the other modes are cooled to the ground state,

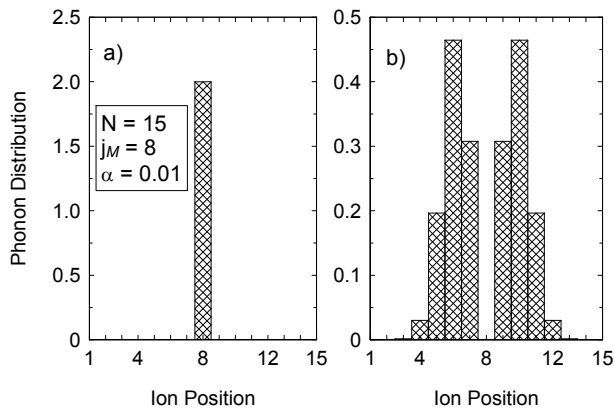


FIG. 3: Average phonon number distribution as described by Eqs. (4) and (7). The impurity ion is placed in the center of a string of $N = 15$ ions, i.e. at position $j_M = 8$. The quantum condensed phase is observed in a heterogeneous ion crystal with fourteen $^{40}\text{Ca}^+$ ions and one $^{43}\text{Ca}^+$ impurity ion, where $n = 2$ collective phonons are localized at the impurity site (a). For $\mu = 40/43$ corresponding to fourteen $^{40}\text{Ca}^+$ ions and one $^{43}\text{Ca}^+$ impurity ion the system is in a quantum conducting phase with non zero phonon distribution (b).

achieving the state $|\Psi\rangle = |00\dots n\rangle$. We find that the average local phonons per site (per ion) $\langle \hat{n}_j \rangle \equiv \langle \Psi | \hat{n}_j | \Psi \rangle$ is given by

$$\langle \hat{n}_j \rangle = \frac{n(b_j^N)^2}{2} \left(\frac{\omega_N}{\omega_x^0} + \frac{\omega_x^0}{\omega_N} \right) + \frac{1}{4} \sum_{k=1}^N (b_j^k)^2 \left(\frac{\omega_k}{\omega_x^0} + \frac{\omega_x^0}{\omega_k} \right) - \frac{1}{2}. \quad (4)$$

First we will discuss the properties of Eq. (4) for $\mu = 1$. The results implies that in general $\sum_j \langle n_j \rangle \geq n$. The inequality does not violate the conservation of energy since the sum of the local phonons energies is decreased due to Coulomb interaction between the ions. However, if α is kept sufficiently small ($\alpha \ll 1$) the transversal vibrational modes are approximately degenerate $\omega_k \approx \omega_x^0$ and the local phonons per site are $\langle n_j \rangle = n(b_j^N)^2$ so that $\sum_j \langle n_j \rangle = n$. In this regime where the Coulomb energy is much weaker than the trapping energy the linear ion crystal is in the quantum conducting (superfluid) phase and the phonon number n is conserved [12]. Now we will discuss the properties of Eq. (4) in the two limits $\mu > 1$ and $\mu < 1$, respectively. As can be seen from Fig. 2b for $\mu > 1$ and $\alpha \ll 1$ all modes are degenerate except $\omega_N = \omega_x^0/\mu$. Moreover, we find that $b_{j_M}^N = 1$ and $b_{j_M}^{k \neq N} = 0$ using Eq. (1). This implies that the heavy ion is oscillating while the others are at rest. The average number of transversal phonons is given by

$$\langle \hat{n}_{j \neq j_M} \rangle = 0, \quad \langle \hat{n}_{j_M} \rangle = n. \quad (5)$$

Thus, for a heavy impurity ion, increasing the number of collective phonons in the LL mode leads to an increase of the average number of local phonons at the impurity site whereas all other ions remain in the vibrational ground state. Hence, the heterogeneous ion crystal is in a quan-

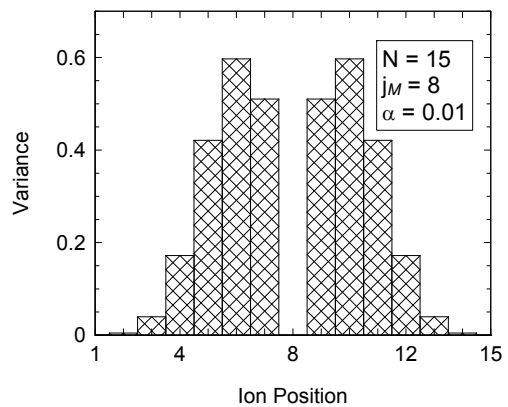


FIG. 4: The variance of the local phonon number operator as described by Eq. (7). The lighter impurity ion is placed in the center of a string of $N = 15$ ions, i.e. at position $j_M = 8$. For $\mu = 40/43$ corresponding to fourteen $^{43}\text{Ca}^+$ ions and one $^{40}\text{Ca}^+$ impurity ion the system is in a quantum conducting phase. The phase is characterized with non-zero variance for all sites except for the impurity ion where the variance is zero.

tum condensed phase where any transversal quantized energy is condensed by the heavy ion.

In the opposite limit of a lighter impurity ion we derive from Eq. (1) that $b_{j_M}^1 = 1$, $b_{j_M}^{k \neq 1} = 0$. Because now only the LL modes are excited, the oscillations of the impurity ion are suppressed and the average number of phonons is

$$\langle \hat{n}_{j \neq j_M} \rangle = n(b_j^N)^2, \quad \langle \hat{n}_{j_M} \rangle = 0. \quad (6)$$

Hence, the lighter impurity ion spreads the phonons to all other ions, such that the heterogeneous ion crystal is in a quantum conducting phase. Eq. (6) shows that the lighter impurity ion is in a vibrational ground state and is independent to the collective phonons n . The phonon distribution is shown in Fig. 3, where both phases are exemplified for the system of a mixed $^{43}\text{Ca}^+ / ^{40}\text{Ca}^+$ crystal.

The different quantum phases become evident also from the variance of the local phonon number operator $\delta n_j = (\langle \hat{n}_j^2 \rangle - \langle \hat{n}_j \rangle^2)^{1/2}$. Again we will start with the case of $\mu = 1$, where we obtain that $\delta n_j = \sqrt{n(b_j^N)^2 - n(b_j^N)^4}$. However, for the heavy impurity case ($\mu > 1$) we derive $\delta n_j = 0$ for all sites. The vanishing phonon variance appears to due the the localization of the collective phonons at the impurity site. If the impurity ion is lighter ($\mu < 1$) we obtain

$$\delta n_{j \neq j_M} = \sqrt{n(b_j^N)^2 - n(b_j^N)^4}, \quad \delta n_{j_M} = 0. \quad (7)$$

Now the variance increases with the amount n of phonons in the LL mode for all ions except for the impurity ion.

Finally, we demonstrate the quantum phases by considering correlations in the number of phonons $C_{ij} = \langle \hat{n}_i \hat{n}_j \rangle - \langle \hat{n}_i \rangle \langle \hat{n}_j \rangle$. For $\mu = 1$ the ion crystal is in the quantum conducting phase with correlation $C_{ij} = -n(b_i^N b_j^N)^2$. Since in the quantum condensed phase

($\mu > 1$) the collective LL phonons are localized at the impurity ion whereas the remaining ions are in the vibrational ground state we find that the correlation C_{ij} for any i and j vanishes. In the quantum conducting phase ($\mu < 1$) the lighter impurity ion is in the vibrational ground state and therefore the correlation C_{ijM} remains zero. However, for all other ions the correlation is $C_{ij} = -n(b_i^N b_j^N)^2$.

To summarize, the impurity doped ion crystal allows to distinguish two quantum phases depends of the mass ratio μ . In the quantum condensed phase ($\mu > 1$) the collective LL phonons are localized at the impurity ion whereas all other ions remain in the vibrational ground state. The localization leads to vanishing of the phonon variance and correlation at all sites. In the quantum conducting phase ($\mu < 1$) the lighter impurity ion is in the vibrational ground state and the collective LL phonons are distributed among the remaining ions. This phase is characterized with non-zero variance and correlation except for the impurity ion.

In the following, we show how to employ an optical dipole force in order to change the effective mass of the impurity ion. In this way μ can be continuously swept through the quantum phase transition.

IV. OPTICAL DIPOLE FORCE

We assume that additionally to the trapping potential an optical dipole force is applied to the impurity ion in the transverse x direction. This force creates a harmonic potential $V_d = M\omega_s^2 \hat{x}_{j_M}^2 / 2$ with frequency ω_s . The total potential is the sum of the two trapping potentials and the Coulomb interaction between the ions. The Hamiltonian for the transverse ion motion is given by [22]

$$\hat{H}(t) = \frac{m}{2} \sum_{j=1}^N \left(\frac{d}{dt} \hat{x}_j \right)^2 + \frac{m(\omega_x^0)^2}{2} \sum_{j,i=1}^N \tilde{B}_{ji} \hat{x}_j \hat{x}_i \quad (8)$$

Here for simplicity we normalize the position operators \hat{x}_j as $\hat{x}_j = \hat{x}_j$ and $\hat{x}_{j_M} = \sqrt{\mu} \hat{x}_j$. Using Eq. (2) the Hamiltonian can be expressed in terms of normal modes as follows

$$\hat{H}(t) = \hat{H}_0 + \frac{1}{2} \sum_{k,q=1}^N \left[m R_{kq} \hat{X}_k \hat{X}_q + S_{kq} (\hat{P}_k \hat{X}_q - \hat{X}_k \hat{P}_q) \right]. \quad (9)$$

The new eigenfrequencies ω_k and eigenvectors b_j^k are obtained by diagonalization of a matrix $\tilde{B}_{ij} = B_{ij} + \beta^2 \delta_{ijM} \delta_{jjM}$, with $\beta = \omega_s / \omega_x^0$. Due to the time-dependent optical dipole interaction the normal modes and momenta are connected by the couplings $R_{kq} = \sum_{j=1}^N \dot{b}_j^k \dot{b}_j^q$ and $S_{kq} = \sum_{j=1}^N b_j^k \dot{b}_j^q$. Here we denote with dot the time derivative, occurring because the magnitude of the dipole force is varied in time.

The experimental scheme starts by preparing the crystal in state $|\Psi\rangle = |00\dots n\rangle$. During an adiabatic increase of the trap potential created by the optical dipole

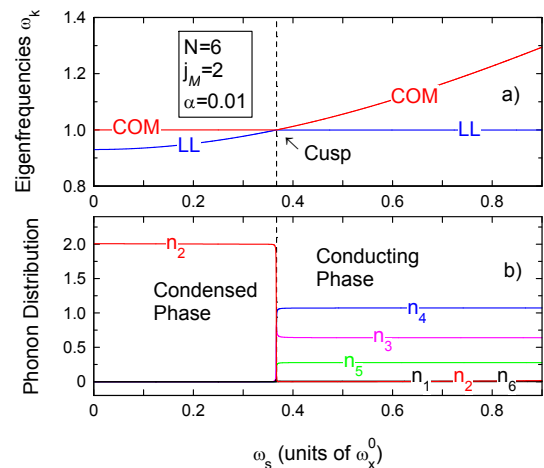


FIG. 5: (color online). (a) The transverse eigenfrequencies ω_k for COM and LL modes as a function of the optical-dipole frequency ω_s for a heterogeneous ion crystal consisting of five $^{40}\text{Ca}^+$ ions and one $^{43}\text{Ca}^+$ impurity ion at the second position. A quantum phase transition is observed by adiabatically sweeping ω_s to higher values. (b) The local average phonon distribution for each ion $\langle \hat{n}_i \rangle = n_i$ ($i = 1, 2, \dots, 6$) as a function of ω_s . As the magnitude of ω_s is changed the mass ratio is reduced and reaches a critical point $\mu_{\text{eff}} = 1$ at which the system undergoes a quantum phase transition from the quantum condensed phase to the quantum conducting phase. The quantum phase transition occurs approximately at $\omega_s = 0.37\omega_x^0$.

force the normal modes become coupled. In order to suppress non-adiabatic transitions to the other modes we require the adiabatic condition to be fulfilled at any instant of time, $|S_{kq}| \ll |\omega_k(t) - \omega_q(t)|$. Then the couplings R_{kq} and S_{kq} can be neglected such that the Hamiltonian (9) describes N uncoupled harmonic oscillators with time-dependent frequencies ω_k . We assume that the frequency of the tightly focused laser field is varying as $\omega_s = \omega_s^0 \sqrt{t}$. The energy spectrum of the linear ion string is now represented by the Demkov-Osherov model [24], which describes the interaction between $N-1$ stationary states and one state varying linearly in time. This allows us to approximate the adiabatic condition as $(\omega_s^0 / \omega_x^0)^2 \lesssim |\omega_k - \omega_q|^2 T$. This condition implies that the temporal energy change should be smaller than the splitting to the next level to avoid transitions. Then the ion crystal remains in the initially prepared state $|\Psi\rangle$ during the adiabatic change of the optical dipole force. To illustrate the effect of the optical force on the transverse spectrum we plot in Fig. 5a the eigenfrequencies ω_k for the COM and LL modes as a function of ω_s for five $^{40}\text{Ca}^+$ ions and one $^{43}\text{Ca}^+$ impurity ion at $j_M = 2$. For sufficiently small $\alpha \ll 1$ the off-diagonal elements of \tilde{B}_{ij} can be neglected and we obtain that the optical dipole force reduces the mass ratio as $\mu_{\text{eff}} = ((\omega_s / \omega_x^0)^2 + 1 / \mu^2)^{-1/2}$. As the magnitude of μ_{eff} is changed, the system reaches a critical point $\mu = 1$ for which the system undergoes a quantum phase transition from the quantum condensed

phase to the quantum conducting phase (see Fig. 5b). Here we assume that the heterogeneous crystal is prepared in a state with $n = 2$ LL collective phonons. In the quantum condensed phase these phonons are localized by the impurity ion with no phonons at the other sites. For sufficiently small α the adiabatic condition requires a long interaction time and high value of ω_s . To avoid this problem we could increase α to 0.1. Then the quantum phase transition occurs approximately at $\omega_s = 2\pi \times 0.4$ MHz and the adiabatic condition is fulfilled within $60 \mu s$. The optical dipole trap can be created by laser detuning up to $\Delta = -2\pi \times 300$ GHz red of the resonance of the $S_{1/2} \leftrightarrow P_{1/2}$ transition of $^{43}\text{Ca}^+$. The frequency ω_s can be achieved by laser power around 350 mW with waist radius of $w_0 = 5 \mu m$.

V. CONCLUSIONS

In conclusion we have presented a realistic scheme for observation of phonon condensation and quantum phase

transition of the transverse local phonons in a heterogeneous ion crystal. Critical behavior appears when the effective mass ratio is changed continuously, which can be achieved by application of light-induced dipole force. The features of the phase transition are clearly visible even for a small number of ions, realizable with the current ion trap technology. Impurity-doped ion crystals offer the advantage that the laser light can be made to interact only with the impurity ion. Moreover, the local phonon mode readout of the impurity ion can be improved by using laser frequencies selectively addressing its sidebands and internal electronic states [13]. The future extension of the proposed technique may use multiple impurity ions for heat, excitation and entanglement transport measurements, investigations of artificial Josephson junctions and separation of phases.

We thank J.I. Cirac and A. Mering for discussions. This work has been supported by the European Commission projects EMALI and MICROTRAP, the Bulgarian NSF grants VU-I-301/07 and D002-90/08, and the Elite programme of the Landesstiftung Baden-Württemberg.

-
- [1] H. Häffner *et al.*, Phys. Rep. **469**, 155 (2008).
 - [2] M. Johanning *et al.*, J. Phys. B: At. Mol. Opt. Phys. **42**, 154009 (2009).
 - [3] F. Schmidt-Kaler *et al.*, Nature **422**, 408 (2003).
 - [4] D. Leibfried *et al.*, Nature **422**, 412 (2003).
 - [5] T. Monz *et al.*, Phys. Rev. Lett. **102**, 040501 (2009).
 - [6] K. Kim *et al.*, Phys. Rev. Lett. **103**, 120502 (2009).
 - [7] S. Gulde *et al.*, Nature **421**, 48 (2003).
 - [8] J. Chiaverini *et al.*, Science **308**, 997 (2005).
 - [9] K.-A. Brickman *et al.*, Phys. Rev. A **72**, 050306 (2005).
 - [10] D. Porras and J. I. Cirac, Phys. Rev. Lett. **92**, 207901 (2004).
 - [11] A. Friedenauer *et al.*, Nat. Phys. **4**, 757 (2008).
 - [12] D. Porras and J. I. Cirac, Phys. Rev. Lett. **93**, 263602 (2004).
 - [13] P. A. Ivanov *et al.*, Phys. Rev. A. **80**(R), 060301 (2009)
 - [14] L. Lamata *et al.*, Phys. Rev. Lett. **98**, 253005 (2007).
 - [15] R. Gerritsma *et al.*, arXiv:0909.0674.
 - [16] T. Rosenband *et al.*, Science **319**, 1808 (2008).
 - [17] M. D. Barrett *et al.*, Phys. Rev. A **68**, 042302 (2003).
 - [18] W. Schnitzler *et al.*, Phys. Rev. Lett. **102**, 070501 (2009).
 - [19] Ch. Schneider *et al.*, arXiv:1001.2953.
 - [20] D. F. V. James, Appl. Phys. B **66**, 181 (1998).
 - [21] D. Leibfried *et al.*, Rev. Mod. Phys. **75**, 281 (2003).
 - [22] D. Kielpinski *et al.*, Phys. Rev. A **61**, 032310 (2000).
 - [23] S. Sachdev, Quantum Phase Transition (Cambridge University Press, Cambridge, England, 1999).
 - [24] Y. N. Demkov and V. I. Osherov, Zh. Eksp. Teor. Fiz. **53**, 1589 (1967) [Sov. Phys. JETP **26**, 916 (1968)].